

Route Swarm: Wireless Network Optimization through Mobility

Ryan K. Williams, Andrea Gasparri, and Bhaskar Krishnamachari

Abstract—In this paper, we demonstrate a novel hybrid architecture for coordinating networked robots in sensing and information routing applications. The proposed *INformation and Sensing driven PhysIcally REconfigurable robotic network (INSPIRE)*, consists of a *Physical Control Plane (PCP)* which commands agent position, and an *Information Control Plane (ICP)* which regulates information flow towards communication/sensing objectives. We describe an instantiation where a mobile robotic network is dynamically reconfigured to ensure high quality routes between static wireless nodes, which act as source/destination pairs for information flow. We demonstrate our propositions through simulation under a realistic wireless network regime.

I. INTRODUCTION

The integration of mobile robotics and wireless networking is an emerging domain with problems ranging from mobile node deployment [1], [2] to ensuring connectivity while performing secondary objectives [3], [4]. Going beyond connectivity, recently, research has also addressed how to control a team of robots to maintain certain desired end-to-end rates while moving robots to do other tasks, referred to as the problem of maintaining network integrity [5]. This is done by interleaving potential-field based motion control and at the higher level an iterative primal-dual algorithm for rate optimization. All of these works point to the need for a hybrid control framework where low-level motion control can be integrated with a higher-level network control plane such as in the architecture we detail in this work.

Specifically, we propose a novel hybrid architecture for command, control, and coordination of networked robots for sensing and information routing applications, called *INSPIRE* (for **INformation and Sensing driven PhysIcally REconfigurable robotic network**). In the *INSPIRE* architecture, we propose two levels of control. At the low level there is a *Physical Control Plane (PCP)*, and at the higher level is an *Information Control Plane (ICP)*. At the *PCP*, iterative local communications between neighboring robots is used to shape the physical network topology by manipulating agent position through motion. At the *ICP*, more sophisticated multi-hop network algorithms enable efficient sensing and information routing (e.g., shortest cost routing computation, time slot allocation for sensor data collection, task allocation, clock synchronization, network localization, etc.). Unlike traditional approaches to distributed

robotics, the introduction of the *ICP* provides the benefit of being able to scalably configure the sensing tasks and information flows in the network in a globally coherent manner even in a highly dynamical context by using multi-hop communications.

As a proof of concept of the *INSPIRE* architecture, we detail an instantiation in which the robotic network is dynamically reconfigured in order to ensure high quality routes between a set of static wireless nodes (i.e. a *flow*) while preserving connectivity, where the number and composition of information flows in the network may change over time. In solving this problem, we propose *ICP* and *PCP* components that couple connectivity-preserving robot-to-flow allocations, with communication optimizing positioning through distributed mobility control; a heuristic we call *Route Swarm*. Finally, we demonstrate our propositions through simulation, illustrating the *INSPIRE* architecture and the *Route Swarm* heuristic in a realistic wireless network regime.

Closely related to our work is an early paper that advocated motion control as a network primitive in optimizing network information flows [6]. Although related in spirit, we provide in this work fundamental advances in flow-to-flow reallocations, dynamic and flexible connectivity maintenance allowing network reconfigurability, and refined potential-based control that requires only inter-agent distance in optimizing intra-flow positioning. Another, more recent work [7], focuses on a single-flow setting, but considers a more detailed fading model communication environment, and a slightly different path metric. In contrast to [7], we make novel contributions in multi-flow optimization which we have shown requires a more sophisticated network-layer information control plane. Moreover, the motion control presented in [7] can also be integrated with and adopted as a component of the *PCP* in the *INSPIRE* architecture presented here.

II. BACKGROUND MATERIAL

A. Agent and Interaction Models

Consider a system of $n = m + s$ agents consisting of m mobile robots indexed by $\mathcal{I}_M \triangleq \{1, \dots, m\}$, and s static sensors indexed by $\mathcal{I}_S \triangleq \{m + 1, \dots, m + s\}$. The mobile robots are assumed to have single integrator dynamics

$$\dot{x}_i = u_i \quad (1)$$

where $x_i, u_i \in \mathbb{R}^2$ are the position and the velocity control input for an agent $i \in \mathcal{I}_M$, respectively. Assume that all agents can intercommunicate in a proximity-limited way, inducing interactions (or topology) of a time varying nature. Specifically, letting $d_{ij} \triangleq \|x_{ij}\| \triangleq \|x_i - x_j\|$ denote the distance between agents i and j , and (i, j) a link between connected agents, the spatial neighborhood of each agent is partitioned by

R. K. Williams and B. Krishnamachari are with the Departments of Electrical Engineering and Computer Science at the University of Southern California, Los Angeles, CA 90089 USA (email: rkwillia@usc.edu; bkrishna@usc.edu).

A. Gasparri is with the Department of Engineering, Roma Tre University, Via della Vasca Navale, 79. Roma, 00146, Italy (email: gasparri@dia.uniroma3.it;).

This work was partially supported by the Italian grant FIRB “Futuro in Ricerca”, project NECTAR, code RBF08QWUV, funded by the Italian Ministry of Research and Education (MIUR).

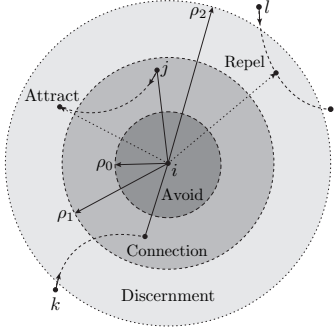


Fig. 1. Agent interaction model with radii $\|x_{ij}\| \leq \rho_2$, neighbor decisions relative to constraints $\rho_1 < \|x_{il}\| \leq \rho_2$, link establishment $\|x_{ik}\| \leq \rho_1$, and collision avoidance $\|x_{ij}\| \leq \rho_0$.

defining concentric radii $\rho_2 > \rho_1 > \rho_0$ as in Fig. 1, where we refer to ρ_2, ρ_1, ρ_0 as the *interaction, connection, and collision avoidance* radii, respectively. The radii introduce a *hysteresis* in interaction by assuming that links (i, j) are established only after $d_{ij} \leq \rho_1$, with link loss then occurring when $d_{ij} > \rho_2$, generating the annulus of $\rho_2 - \rho_1$ where *decisions* on link additions and deletions are made (c.f. Section IV-A).

The above spatial interaction model is formalized by the *undirected dynamic graph*, $\mathbb{G} = (\mathcal{V}, \mathcal{E})$, with vertices (nodes) \mathcal{V} indexed by $\mathcal{I}_M \cup \mathcal{I}_S$ (the agents), and edges $\mathcal{E} \subseteq \mathcal{V} \times \mathcal{V}$ such that $(i, j) \in \mathcal{E} \Leftrightarrow (\|x_{ij}\| \leq \rho_2) \wedge \sigma_{ij}$, with switching signals [8]:

$$\sigma_{ij} = \begin{cases} 0, & (i, j) \notin \mathcal{E} \wedge \|x_{ij}\| > \rho_1 \\ 1, & \text{otherwise} \end{cases} \quad (2)$$

where $(i, i) \notin \mathcal{E}$ (no self-loops) and $(i, j) \in \mathcal{E} \Leftrightarrow (j, i) \in \mathcal{E}$ (symmetry) hold for all $i, j \in \mathcal{V}$. Nodes with $(i, j) \in \mathcal{E}$ are called *neighbors* and the neighbor set for an agent i is denoted $\mathcal{N}_i = \{j \in \mathcal{V} \mid (i, j) \in \mathcal{E}\}$.

B. Assumptions and Problem Formulation

From the set of static sensors \mathcal{I}_S we construct f *information flows* indexed by $\mathcal{I}_F \triangleq \{n+1, \dots, n+f\}$, each consisting of source-destination pairs defining a desired flow of network information. For a given flow $i \in \mathcal{I}_F$, we use the following notation: $\mathcal{F}_i \in \mathcal{I}_S \times \mathcal{I}_S$ represents the source and destination nodes for flow i , with $\mathcal{F}_i^s \in \mathcal{I}_S$ and $\mathcal{F}_i^d \in \mathcal{I}_S$ representing source and destination indices, respectively. Further, for convenience we use notation $x_i^s, x_i^d \in \mathbb{R}^2$ to represent the position of the source and destination for the flow $i \in \mathcal{I}_F$. The set of flow pairs is denoted $\mathcal{F} \triangleq \{\mathcal{F}_1, \dots, \mathcal{F}_f\}$. At any time, a subset of these static pairs is active, forming the set of active flows \mathcal{I}_F , calling for dynamic configurability of the hybrid network, our contribution in this work. Thus, at a high level our system objective is to facilitate information flow for each source/destination pair by configuring the mobile robots such that each flow is *connected* and is at least approximately optimal in terms of data transmission, and that the entire network itself \mathbb{G} is connected to guarantee complete network collaboration.

Assumption 1 (Connectedness). It is assumed that the locations of the static nodes and the cardinality of mobile nodes is

such that the set of connected graphs \mathbb{G} that could be formed is non-empty, and that their communication graph is initiated to be in this set.

To measure link quality towards optimizing a given flow, we assume that each $(i, j) \in \mathcal{E}$ has a weight parameter w_{ij} that describes their cost with respect to transmitting information. A commonly used metric for link quality is *ETX*, i.e. the expected number of transmissions per successfully delivered packet. This can be modeled as the inverse of the successful packet reception rate λ_{ij} over the link. As the expected packet reception rate has been empirically observed and analytically shown to be a sigmoidal function of distance decaying from 1 to 0 as distance d_{ij} is increased [9], it can be modeled as follows:

$$\lambda_{ij} \approx 1 - \frac{1}{(1 + e^{-a(d_{ij}-b)})} \quad (3)$$

where $a, b \in \mathbb{R}_+$ are shape and center parameters depending on the communication range and the variance of environmental fading. Accordingly, the link weights w_{ij} , if chosen to represent ETX, can be modeled as a convex function of the inter-node distance d_{ij} :

$$w_{ij} = \frac{1}{\lambda_{ij}} = \frac{1}{1 - \frac{1}{1 + e^{-a(d_{ij}-b)}}} = 1 + e^{a(d_{ij}-b)} \quad (4)$$

The cost for flow $k \in \mathcal{I}_F$ is then taken to be the sum of ETX values on the path of the flow, i.e.:

$$W_k = \sum_{(i,j) \in \mathcal{E}_F^k} w_{ij} \quad (5)$$

where we apply notation $\mathbb{G}_F^k = (\mathcal{V}_F^k, \mathcal{E}_F^k)$ as the graph defining the interconnection over flow $k \in \mathcal{I}_F$ (we give a concrete definition of flow *membership* in Section III-A). Our problem in this work is then formalized as follows:

Problem 1 (Multi-flow optimization). The network-wide goal then is to find an allocation and configuration of mobile agents so as to minimize the total cost function¹ $\sum_{k=1}^f W_k$ while maintaining both intra-flow connectivity (to guarantee information delivery) and inter-flow connectivity (to guarantee flow-to-flow information passage/collaboration).

III. INFORMATION CONTROL PLANE (ICP)

There are two key elements in solving Problem 1: on the one hand, within a given flow $k \in \mathcal{I}_F$, for a given allocation of a certain number of mobile nodes to that flow, node configuration should minimize the flow cost W_k . On the other hand, the number of mobile nodes allocated to each flow should minimize the overall cost $\sum_k W_k$. We first consider these optimizations ideally, in the absence of connectivity constraints. The first, per-flow element of the network optimization dictates the desired spatial configuration of allocated mobile nodes within a flow.

Theorem 1 (Equidistant optima). *For a fixed number of mobile nodes $m_k \triangleq |\mathcal{V}_F^k|$ allocated to a given flow and arranged on*

¹The negative of the cost could be treated as a utility function. We therefore equivalently talk about cost minimization or utility maximization.

the line between the source and destination of that flow, the arrangement which minimizes (5) is one where the nodes are equally spaced.

Proof. This follows from the following general result: to minimize a convex $y(\vec{z})$ s.t. $\sum z_i = c$, the first order condition (setting the partial derivative of the Lagrangian with respect to each element z_i to 0) yields that $\frac{\partial y}{\partial z_i} = \mu$ where μ is the Lagrange multiplier. Now if $\frac{\partial y}{\partial z_i}$ is the same for all z_i , then the solution to this optimization is to set $z_i = \frac{c}{|z|}$, i.e. all variables are made to be the same.

The z_i in the above correspond to the inter-node distances d_{ij} , and the y corresponds to (5). Since w_{ij} is a convex function of distance between neighboring nodes, the path metric W_k is a convex function of the vector of inter-node distances. Further, since the sum of all inter-node distances is the total distance between the source and destination of the flow, which are static, it is constrained to be a constant d_k . Since the weight of each link is the same function of the inter-node distance, $\frac{\partial W_k}{\partial d_{ij}}$ is the same for all pairs of neighboring nodes. Therefore the intra-flow optimization (i.e., choosing node positions to minimize W_k) is achieved by a equal spacing of the nodes. \square

The second, global cross-flow element of the network optimization dictates the number of mobile nodes allocated to each flow. The goal is to minimize the total network cost $\sum_k W_k$. Our approach to solving this optimization is motivated by the following observation: When the intra-flow locations of the robots are optimized to be equally spaced, W_k is a function of the number of nodes m_k allocated to flow k , and the total number of nodes allocated to all flows is constrained by the total number of mobile nodes. If we could show that W_k is a convex function, then to minimize the total network cost we need to identify the allocation at which the marginal costs for all flows are as close to equal as possible (ideally, if m_k was a continuous quantity, they would all be equal at the optimum point, but due to the discrete nature of m_k this is generally not possible).

In the following, for ease of analysis, we consider the continuous relaxation of the problem, allowing m_k to be a real number, and hence W_k to be a continuous function.

Theorem 2 (Convexity). *For any flow k that has been optimized to have the lowest possible cost W_k (i.e. all m_k mobile nodes are equally spaced), W_k is a convex function of m_k .*

Proof. The theorem can be proven as follows:

$$W_k = (m_k + 1)w\left(\frac{d_k}{m_k + 1}\right) \quad (6)$$

$$\Rightarrow W'_k = w\left(\frac{d_k}{m_k + 1}\right) - \frac{d_k}{m_k + 1}w'\left(\frac{d_k}{m_k + 1}\right) \quad (7)$$

$$\Rightarrow W''_k = w''\left(\frac{d_k}{m_k + 1}\right)\frac{d_k^2}{(m_k + 1)^3} \quad (8)$$

Since the link weight function $w(\cdot)$ is a convex function of the internode distance, we have that $w''\left(\frac{d_k}{m_k + 1}\right)$ is positive, and therefore we have that W''_k is positive, hence W_k is convex in m_k . \square

Note that in reality m_k is a discrete quantity, but the above argument suffices to show that W_k is a discrete convex function of m_k (since convexity over a single real variable implies discrete convexity over the integer discretization of the variable).

Theorem 3 (Optimality). *The problem of minimizing $\sum_k W_k(m_k)$ subject to a constraint on $\sum_k m_k$ can be solved optimally in an iterative fashion by the following greedy algorithm: at each iteration, move one node from the flow where its removal induces the lowest increase in cost to the flow where its addition would yield the highest decrease in cost, so long as the latter's decrease in cost is strictly higher in absolute value than the former's increase in cost (i.e. so long as the move serves to reduce the overall cost).*

We omit the detailed proof due to space constraint, but intuitively, this algorithm works by moving the system iteratively towards the optimum by following the steepest gradient in terms of cost reduction for the movement of each node. Since the overall optimization problem is convex, there is only a single optimum, to which this algorithm will converge. Moreover, since there is a strict improvement in each step and there are a finite number of nodes, the algorithm reaches the optimal arrangement in a finite number of steps.

Thus far, we have described both the intra-flow and inter-flow optimization problems in an ideal setting where both problems are convex optimization problems and as such can be solved exactly. However, in the robotic system we are considering there is one significant source of non-ideality/non-convexity, which is that the network must be maintained at all times in a connected configuration. This has two consequences. First, some of the mobile nodes may be needed as *bridge* nodes that do not participate in any flow and are instead used to maintain connectivity across flows. Second, the locations of some of the nodes even within each flow may be constrained in order to maintain the connectivity requirement. The solution for the constrained problem therefore may not correspond exactly to the solutions of the ideal optimization problems described above.

We therefore develop a heuristic solution that we refer to as *Route Swarm*, which is inspired by and approximates the ideal optimizations above but is adapted to maintain connectivity. Route Swarm has both an intra-flow and inter-flow component. As per the INSPIRE architecture, the intra-flow function is performed by the PCP, while the inter-flow function is performed by ICP. The ICP algorithm, shown as pseudocode as Algorithm 1, approximates the ideal iterative optimization described above by allocating mobile robots between flows greedily on the basis of greatest cost-reduction; to handle the inter-flow connectivity constraint, it incorporates a subroutine (Algorithm 2) to detect which nodes are not mobile because they must act as bridge nodes. Moreover, it also allocates any nodes that are no longer required to support an inactive flow to join active flows. And within each flow, the PCP algorithm attempts to keep the robots as close to evenly spaced as possible while taking into account the inflexibility of the bridge nodes. The details of the route swarm algorithm are given below.

Algorithm 1 ICP optimization algorithm.

```

1: procedure INFORMATIONCONTROLPLANE
2:   ▷ Detect initial flow members based on shortest paths:
3:   for  $i \in \mathcal{I}_F$  do
4:      $\mathcal{M} \leftarrow \text{SHORTESTPATH}(\mathbb{G}, \mathcal{F}_i)$ 
5:   end for
6:   ▷ Detect flow-to-flow bridges for connectivity:
7:    $b \leftarrow \text{DETECTBRIDGES}(\mathbb{G}, \mathcal{F}, \mathcal{M})$ 
8:   ▷ Detect best connectivity-preserving flow detachment:
9:    $d \leftarrow \text{BESTDETACHMENT}(\mathbb{G}, \mathcal{F}, \mathcal{M}, b)$ 
10:  ▷ Compute flow attachment with most utility:
11:   $a \leftarrow \text{BESTATTACHMENT}(\mathcal{F}, \mathcal{M})$ 
12:  ▷ Ensure optimizing reconfiguration exists (weighted by  $\beta \in \mathbb{R}_+$ ):
13:  if  $a > \beta d$  then
14:    ▷ Optimal command is best detach/attach pair:
15:    return  $\mathcal{C}_d \leftarrow a$ 
16:  end if
17: end procedure

```

Algorithm 2 ICP bridge detection.

```

1: procedure DETECTBRIDGES( $\mathbb{G}, \mathcal{F}, \mathcal{M}$ )
2:   ▷ Initialize supergraph with nodes for each flow:
3:    $\mathbb{S} \leftarrow (\{i \in \mathcal{I}_F\}, \emptyset)$ 
4:   ▷ Append nodes/edges for non-flow members:
5:    $\mathbb{S} \leftarrow \text{ADDFLOWMEMBERS}(\mathbb{S}, \mathcal{F}, \mathcal{M})$ 
6:   ▷ Append edges for flow members:
7:    $\mathbb{S} \leftarrow \text{ADDNONFLOWMEMBERS}(\mathbb{S}, \mathcal{F}, \mathcal{M})$ 
8:   ▷ Bridges lie on shortest path between all flow pairs:
9:   return  $b \leftarrow \text{SHORTESTPATHS}(\mathbb{S}, \mathcal{F})$ 
10: end procedure

```

A. The Route Swarm Heuristic

In solving the connectivity constrained version of the flow optimization of Theorems 1, 2, and 3, due to problem complexity we provide a heuristic algorithm to solve the inter-flow allocation problem, leaving the intra-flow optimization to the PCP (Section IV). Algorithm 1 depicts the high-level components of the proposed heuristic, each of which is detailed in the sequel.

To begin, we define the flow membership for an agent as $i \in \mathcal{I}_M$ as $\mathcal{M}_i \in \mathcal{I}_F$, where the set of memberships is denoted as $\mathcal{M} \triangleq \{\mathcal{M}_1, \dots, \mathcal{M}_n\}$. We denote with $\mathbb{G}_F^i = (\mathcal{V}_F^i, \mathcal{E}_F^i)$ the graph defining the interconnection over flow $i \in \mathcal{I}_F$ of agents $j \in \mathcal{I}_S \cup \mathcal{I}_M$ with $i \in \mathcal{M}_j$. Thus we have $\mathcal{V}_F^i = \{j \in \mathcal{I}_S \cup \mathcal{I}_M \mid i \in \mathcal{M}_j\}$ and $(j, k) \in \mathcal{E}_F^i \Leftrightarrow (i \in \mathcal{M}_j \cap \mathcal{M}_k) \wedge (j \in \mathcal{N}_k)$, with $k \in \mathcal{I}_S \cup \mathcal{I}_M$. Notice that by definition $\mathbb{G}_F^i \subseteq \mathbb{G}$. We will also refer to the collection of flow graphs simply by \mathbb{G}_F . We also have flow neighbors defined as $\mathcal{N}_i^F = \{j \in \mathcal{N}_i \mid \mathcal{M}_j \cap \mathcal{M}_i \neq \emptyset\}$. Furthermore, we denote with $\mathcal{D}_i \in \mathcal{I}_M$ the detachable agents $j \in \mathcal{I}_M$ for flow $i \in \mathcal{I}_F$, i.e. those agents for which reconfiguration does not impact network connectedness. The set of detachments is denoted by $\mathcal{D} \triangleq \{\mathcal{D}_1, \dots, \mathcal{D}_f\}$.

Due to the system connectivity constraint, the ICP is not free to select *any* mobile agent for flow reallocation, specifically as intra-flow connectivity or overall flow-to-flow connectivity may be lost. Thus, the ICP must detect *bridges*, i.e., mobile nodes whose reconfiguration might break flow-to-flow connectivity over the network, and also consider *safe detachments* (flow-to-flow motion), i.e., a node whose reconfiguration in the workspace does not impact the connectivity of the source flow.

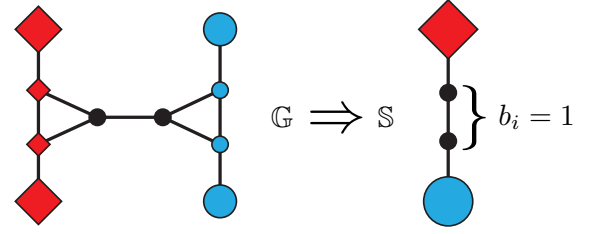


Fig. 2. Example supergraph construction for a network with $f = 2$ flows, $s = 4$ static nodes, and $m = 6$ mobile robots. Flow membership is denoted by color and node shape. Notice that a multi-hop bridge is detected via the shortest path between flows.

Respecting our connectivity constraint, we first detect initial flow membership by computing the shortest path (in terms of link cost) for each source/destination pair per flow by using for example Dijkstra’s algorithm (lines 3-5 of Algorithm 1). This defines the connected *backbone* for each flow implicitly identifying the mobile nodes required to maintain flow-connectivity. Additionally, we have optimality of the connected flow backbones as we maximize the link utility (or minimize path costs) between source and destination nodes.

In detecting bridge agents we follow the process outlined by Algorithms 2, 3, and 4, where we denote by $b_i \in \{0, 1\}$ the status of agent $i \in \mathcal{I}_S \cup \mathcal{I}_M$ as a connectivity preserving bridge, with $b = \{b_1, \dots, b_n\}$. Briefly speaking, the primary problem of this process is the construction of a *supergraph*, denoted $\mathbb{S} = (\mathcal{V}_S, \mathcal{E}_S)$, defining the interconnection of the flows. In this way, we can identify nodes which are critical in defining the flow-to-flow connectivity over the system. Figure 2 depicts an example of supergraph construction. We first add one node for each flow in the system, and then we add a node for each non-flow member in the system that represents potential bridge candidates. Edges between non-flow members are preserved, while there is only one edge between any given non-flow member and the node which represents a flow in the supergraph. Bridges can then be simply detected as the members of the shortest path between any pair of nodes representing flows in the supergraph (e.g. Fig. 2), where connectivity is guaranteed by construction:

Proposition 1 (Bridge detection). *Consider the graph $\mathbb{G}_c \subseteq \mathbb{G}$ obtained by including all the flow-members for any flow and the non-flow members belonging to any shortest path of the supergraph \mathbb{S} . Then \mathbb{G}_c is a spanning-graph representing a connected component of the graph \mathbb{G} .*

Proof. In order to prove this result we must show that both intra-flow and inter-flow connectedness is ensured. The former follows directly from the flow-membership definition while the latter follows from the connectedness between any pair of flows. \square

After identifying the bridge agents that maintain flow-to-flow connectivity and the safely detachable agents per-flow (those which are not on the backbone), the ICP issues reconfiguration commands $\mathcal{C}_i \in \mathcal{I}_F$ to mobile agents $i \in \mathcal{I}_M$ indicating a desired flow membership towards optimizing inter-flow agent allocation. Specifically, as detailed in Algorithms 5 and 6, and

Algorithm 3 ICP supergraph non-flow member nodes/edges.

```
1: procedure ADDNONFLOWMEMBERS( $\mathbb{S}, \mathcal{F}, \mathcal{M}$ )
2:    $\triangleright$  Add nodes for each non-leaf, non-flow member:
3:    $\mathcal{V}_+ \leftarrow \{i \in \mathcal{I}_M \mid (\mathcal{M}_i = \emptyset) \wedge (\mathcal{N}_i \geq 2)\}$ 
4:    $\mathcal{V}_\mathbb{S} \leftarrow \mathcal{V}_\mathbb{S} \cup \mathcal{V}_+$ 
5:    $\triangleright$  Add edges between non-flow members:
6:    $\mathcal{E}_\mathbb{S} \leftarrow \mathcal{E}_\mathbb{S} \cup \{(i, j) \mid (i, j \in \mathcal{V}_+) \wedge (j \in \mathcal{N}_i)\}$ 
7:    $\triangleright$  Add non-flow member to flow member edges:
8:    $\mathcal{E}_\mathbb{S} \leftarrow \mathcal{E}_\mathbb{S} \cup \{(i, j) \mid (i \in \mathcal{V}_+) \wedge (j \in \mathcal{N}_i) \wedge (\mathcal{M}_j \neq \emptyset)\}$ 
9:   return  $\mathbb{S}$ 
10: end procedure
```

Algorithm 4 ICP supergraph flow member edges.

```
1: procedure ADDFLOWMEMBERS( $\mathbb{S}, \mathcal{F}, \mathcal{M}$ )
2:    $\triangleright$  Add edges due to multiple flow memberships:
3:   for  $i \in \mathcal{I}_M \mid |\mathcal{M}_i| \geq 2$  do
4:      $\triangleright$  Add an edge for every membership pair:
5:      $\mathcal{E}_\mathbb{S} \leftarrow \mathcal{E}_\mathbb{S} \cup \{(i, j) \mid j \in \mathcal{I}_F \cap \mathcal{M}_i\}$ 
6:   end for
7:   return  $\mathbb{S}$ 
8: end procedure
```

as motivated by Theorem 3, we compute the safe detachment having the least in-flow utility, and couple it with the flow attachment (i.e. the addition of a contributing flow member) which improves most in terms of link utility and flow alignment (the primary contributions a mobile agent can have in information flow). This decision, if feasible (utility of attachment outweighs cost of detachment), is then passed to the PCP to execute the mobility necessary for reconfiguration, achieving our goal of dynamic utility improving and connectivity preserving network configurations.

IV. PHYSICAL CONTROL PLANE (PCP)

The complementary component to the ICP in the INSPIRE architecture is the PCP which coordinates via state feedback, i.e. $\{\mathbf{x}, \mathbb{G}, \mathbb{G}_F\}$, to generate swarming behaviors that optimize the network dynamically in response to ICP commands. Our desire for generality in coordinating behaviors dictates that the PCP takes on a *switching* nature, associating a distinct *behavior controller* with each of a finite set of discrete agent states. Specifically, define

$$\mathcal{S}_i \in \mathbb{B} \triangleq \{\text{SWARMING}, \text{RECONFIGURE}\} \quad (9)$$

as the *behavior state* of a mobile robot $i \in \mathcal{I}_M$, where \mathbb{B} is the space of discrete agent behaviors. Here, when $\mathcal{S}_i = \text{SWARMING}$, agent i acts to optimize its assigned flow \mathcal{M}_i . Otherwise, when $\mathcal{S}_i = \text{RECONFIGURE}$, agent i traverses the workspace fulfilling global allocation commands \mathcal{C}_i from the ICP. Each component comprising the PCP switching is detailed in the sequel.

A. Constraining Agent Interaction

In order to control the properties of \mathbb{G} (i.e. connectivity) we exploit the *constrained interaction* framework proposed in [10]. The constrained interaction framework acts through hysteresis (2) to regulate links *spatially* with simple application of attraction and repulsion to retain established links or reject new links with respect to topological constraints. Define

Algorithm 5 ICP best flow detachment.

```
1: procedure BESTDETACHMENT( $\mathbb{G}, \mathcal{F}, \mathcal{M}, b$ )
2:    $\triangleright$  Non-member, non-bridges are detachable:
3:   for  $(i \in \mathcal{I}_M) \wedge (\mathcal{M}_i = \emptyset) \wedge (-b_i)$  do
4:      $j \leftarrow$  Flow most contributed to by agent  $i$  (utility)
5:      $\mathcal{M}_i \leftarrow j$ 
6:      $\mathcal{D}_j \leftarrow \mathcal{D}_j \cup i$ 
7:   end for
8:    $\triangleright$  Best detachment has least in-flow utility:
9:   return  $\text{argmin}_{i \in \mathcal{D}} (\sum_{j \in \mathcal{N}_i^F} w_{ij})$ 
10: end procedure
```

Algorithm 6 ICP best flow attachment.

```
1: procedure BESTATTACHMENT( $\mathcal{F}, \mathcal{M}$ )
2:    $\triangleright$  Determine utility of attachment per flow:
3:   for  $i \in \mathcal{I}_F$  do
4:      $\triangleright$  Weigh added node utility against flow path alignment:
5:      $a_i \leftarrow (|\mathcal{V}_F^i| + 1) \sum_{j \in \mathcal{V}_F^i} 1/\|x_j - 1/2(x_i^s + x_i^d)\|$ 
6:   end for
7:   return  $\text{argmax}_{i \in \mathcal{I}_F} (a_i)$ 
8: end procedure
```

the *discernment region* $\|x_{ij}\| \in (\rho_1, \rho_2]$, where agent i decides relative to system constraints (here connectivity) whether agent j is a *candidate* for link addition ($j \notin \mathcal{N}_i$) or deletion ($j \in \mathcal{N}_i$), or if agent j should be attracted (retain $(i, j) \in \mathcal{E}$) or repelled (deny $(i, j) \notin \mathcal{E}$). Define *predicates* for link addition and deletion, $P_{ij}^a, P_{ij}^d: \mathcal{V} \times \mathcal{V} \rightarrow \{0, 1\}$, activated at ρ_2 and ρ_1 , respectively, that indicate constraint violations if the link (i, j) were allowed to be either created or destroyed, i.e. $\|x_{ij}\|$ transits ρ_1 or ρ_2 . The predicates designate for the i th agent the membership of nearby agents in link addition and deletion candidate sets $\mathcal{C}_i^a, \mathcal{C}_i^d$, and attraction and repulsion sets $\mathcal{D}_i^a, \mathcal{D}_i^r$. Link control is then achieved by choosing control u_i having attractive and repulsive *potential fields* between members of $\mathcal{D}_i^a, \mathcal{D}_i^r$, respectively.

In particular, to regulate network topology spatially, we design the agent controls as follows:

$$u_i = u_i^e + u_i^o - \nabla_{x_i} \left(\sum_{j \in \mathcal{D}_i^a} \psi_{ij}^a + \sum_{j \in \mathcal{D}_i^r} \psi_{ij}^r + \sum_{j \in \Pi_i} \psi_{ij}^c \right) \quad (10)$$

with *potentials* $\psi_{ij}^a, \psi_{ij}^r, \psi_{ij}^c: \mathbb{R}_+ \rightarrow \mathbb{R}_+$, serving the purposes of attraction, repulsion, and collision avoidance, where $\Pi_i = \{j \in \mathcal{V} \mid \|x_{ij}\| \leq \rho_0\}$ is the collision avoidance set for agent i . Further, each agent can also apply (based on \mathcal{S}_i) an exogenous objective (i.e. non-cooperative) controller $u_i^e \in \mathbb{R}^2$ and an inter-agent coordination objective $u_i^o \in \mathbb{R}^2$ (e.g. dispersion as will be seen in Section IV-D). The attractive and repulsive potentials are constructed such that $\psi_{ij}^a \rightarrow \infty$ as $d_{ij} \rightarrow \rho_2$ and $\psi_{ij}^r \rightarrow \infty$ as $d_{ij} \rightarrow \rho_1$, guaranteeing link retention and denial, respectively, and allowing us through predicates P_{ij}^a, P_{ij}^d to control desired properties of \mathbb{G} (e.g. connectivity).

B. Connectivity Maintenance

Notice that in *maintaining* network connectivity, we require *only* link retention action, allowing us to immediately choose

$$P_{ij}^a \triangleq 0, \quad \forall i \in \mathcal{I}_M, j \in \mathcal{I}_M \cup \mathcal{I}_S, (\mathcal{S}_i, \mathcal{S}_j) \in \mathbb{B} \times \mathbb{B} \quad (11)$$

for the link addition predicates, effectively allowing link additions to occur between all interacting agents across all network states². Now, the link deletion predicates are given by:

$$P_{ij}^d \triangleq \begin{cases} 1, & (\mathcal{S}_i \vee \mathcal{S}_j = \text{SWARMING}) \wedge \\ & ((\mathcal{M}_i \cap \mathcal{M}_j \neq \emptyset) \vee (b_i \vee b_j = 1)) \\ 0, & \text{otherwise} \end{cases} \quad (12)$$

where by assumption $i, j \in \mathcal{I}_M$, i.e. only mobile agents apply controllers. We choose link retention (12) to guarantee that connectivity is maintained both within flows across \mathbb{G}_F , and from flow to flow across bridge agents over the supergraph \mathbb{S} , noting that idle agents with $\mathcal{M}_i = \emptyset$ and reconfiguring agents with $\mathcal{S}_i = \text{RECONFIGURE}$ are free to lose links as they have been deemed redundant by the ICP with respect to network connectivity.

C. Flow Reconfiguration Maneuvers

While maintaining connectivity as above, each agent further acts according to ICP reconfiguration commands towards optimizing inter-flow allocations. Specifically, in response to command \mathcal{C}_i , agent i enters the reconfiguration state $\mathcal{S}_i \leftarrow \text{RECONFIGURE}$, and begins to apply a *waypoint* controller as follows. When $\mathcal{S}_i = \text{RECONFIGURE}$, agent i applies exogenous objective controller

$$u_i^e \triangleq \frac{x^w - x_i}{\|x^w - x_i\|} - \dot{x}_i \quad (13)$$

where $x^w \in \mathbb{R}^2$ is the target waypoint calculated as the midpoint of target flow \mathcal{C}_i . The input (13) is a velocity damped waypoint seeking controller, having unique critical point $x_i \rightarrow x^w$ (i.e. a point at which $u_i^e = \mathbf{0}$), guaranteeing that the target intra-flow positioning (and thus membership) for agent i is achieved. As the convergence of $x_i \rightarrow x^w$ is asymptotic in nature, to guarantee finite convergence and state switching, we apply a saturation $\|x^w - x_i\| \leq \epsilon^w$ with $0 < \epsilon^w \ll 1$ to detect waypoint convergence, initiating a switch to $\mathcal{S}_i \leftarrow \text{SWARMING}$.

D. Intra-Flow Controllers

Once the ICP has assigned flow memberships $\mathcal{M}_i \forall i \in \mathcal{I}_M$ and all *commanded* reconfigurations \mathcal{C}_i have been completed, the mobile agents begin to seek to optimize the flow to which they are a member. First, we assume that flow members must configure along the line segment connecting flow source/destination pairs, yielding in the case of proximity-limited communication, a line-of-sight or beamforming style heuristic. The membership of an agent $i \in \mathcal{I}_M$ to a flow $j \in \mathcal{M}_i$ thus initiates a check to determine if x_i lies on the flow path $x_j^s + \tau x_j^d$, within a margin $0 < \epsilon_F \ll 1$. To do so, the projection of x_i onto $x_j^s + \tau x_j^d$ is determined first by computing

$$\tau \triangleq \frac{(x_i - x_j^s) \cdot (x_j^d - x_j^s)}{\|x_j^d - x_j^s\|^2} \quad (14)$$

²Although in this work we allow all link additions, link addition control could be useful for example in regulating neighborhood sizes to mitigate spatial interference, or to disallow interaction between certain agents.

defining whether the projection will lie within or outside of the flow path. Then we have the saturated projection

$$x_{i \rightarrow \mathcal{F}_j} = \begin{cases} x_j^s - \alpha\tau(x_j^d - x_j^s), & \tau < 0 \\ x_j^d - \alpha\tau(x_j^d - x_j^s), & \tau > 1 \\ x_j^s + \tau(x_j^d - x_j^s), & \tau \in (0, 1) \end{cases} \quad (15)$$

where $\alpha > 0$ is a biasing term such that the projection does not intersect x_j^s or x_j^d . We then have the state transition condition

$$\|x_{i \rightarrow \mathcal{F}_j} - x_i\| \leq \epsilon_F \quad (16)$$

which when satisfied gives $\mathcal{S}_i \leftarrow \text{SWARMING}$. If condition (16) is not satisfied, agent i transitions to state $\mathcal{S}_i \leftarrow \text{RECONFIGURE}$, applying waypoint controller (13) with $x^w \triangleq x_{i \rightarrow \mathcal{F}_j}$, guaranteeing a reconfiguration, in a shortest path manner, to a point on the line segment defining its assigned flow \mathcal{M}_i .

Finally, when an agent i is in the swarming state $\mathcal{S}_i = \text{SWARMING}$, after all necessary reconfigurations have been made (either by the ICP via \mathcal{C}_i or internally by flow alignment), a *dispersive* inter-neighbor controller is applied in order to optimize the assigned flow. Specifically, each swarming agent $i \in \mathcal{I}_M$ applies a coordination controller (regardless of bridge status b_i):

$$u_i^o \triangleq -\nabla_{x_i} \sum_{j \in \mathcal{N}_i^A} \frac{1}{\|x_{ij}\|^2} - \sum_{j \in \mathcal{N}_i^S} \nabla_{x_j} \frac{1}{\|x_{ji}\|^2} \quad (17)$$

where

$$\mathcal{N}_i^A \triangleq \{j \in \mathcal{N}_i \mid (\mathcal{M}_j \cap \mathcal{M}_i \neq \emptyset) \wedge [(\mathcal{S}_j = \text{SWARMING}) \vee (j \in \mathcal{I}_S)]\} \quad (18)$$

is the set of neighbors that share membership in flow \mathcal{M}_i , and who are either *in flow* and *actively* swarming (i.e. by condition (16)), or are a static source/destination node. Further, we define

$$\mathcal{N}_i^S \triangleq \{j \in \mathcal{N}_i^A \mid j \in \mathcal{I}_S\} \quad (19)$$

as the set of static in flow neighbors for which compensation must be applied. Controller (17) dictates that mobile flow members disperse equally only with fellow flow members and also with the source/destination nodes of their assigned flow \mathcal{M}_i .

While dispersive controllers generally yield equilibria in which inter-agent distant is maximized (up to ρ_2) [11], as each flow is constrained by static source/destination nodes, the dispersion (17) generates our desired equidistant intra-flow configuration as given below:

Proposition 2 (Equidistant dispersion). *Consider the application of coordination objective (17) to a set of mobile agents $i \in \mathcal{I}_M$ within the context of interaction controller (10), each sharing membership to a flow $k \in \mathcal{I}_F$, i.e. $\mathcal{M}_i = k, \forall i$. It follows that at equilibrium the agents are configured such that the equidistant spacing condition*

$$\|x_{ij}\| \rightarrow \frac{\|x_k^d - x_k^s\|}{|\mathcal{V}_F^k| - 1}, \quad \forall i \mid j \in \mathcal{N}_i^F \quad (20)$$

holds asymptotically over flow k .

A formal proof is beyond the scope of this work, however note that our controllers operate using *only* inter-agent distance, an advancement beyond related works such as [6].

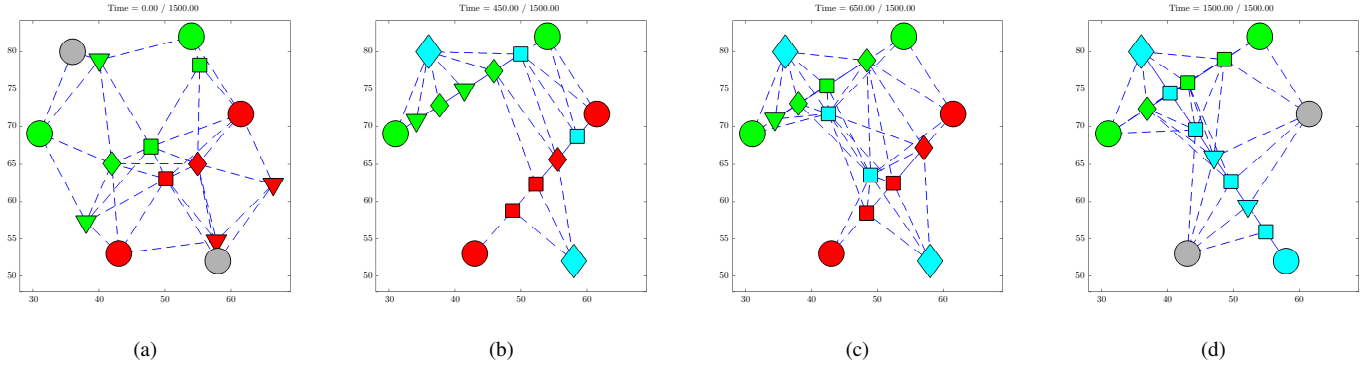


Fig. 3. Flow membership is indicated by color, where square nodes are the flow backbone, triangle nodes are redundant with respect to connectivity, and diamond nodes are bridges. Note that flow \mathcal{F}_3 is initially inactive and becomes active at $t = 450$, while \mathcal{F}_2 is initially active and deactivates at $t = 850$.

V. SIMULATION RESULTS

In this section, we present a simulated execution of our described INSPIRE proof-of-concept, Route Swarm. Consider a system operating over a workspace in \mathbb{R}^2 , having $n = 15$ total agents, $m = 9$ of which are mobile and $s = 6$ of which are static information source/destinations. Assume we have $f = 3$ flows (green, red, and blue indicate flow membership), with the initial system configuration depicted as in Fig. 3a (notice that \mathbb{G} is initially connected), with the system dynamics shown in Fig. 3b through 3d. We simulate a scenario in which \mathcal{F}_3 is initially *inactive* (gray), allowing the ICP to optimize agent allocation over only $f = 2$ flows. By Fig. 3b, flows \mathcal{F}_1 and \mathcal{F}_2 have been assigned an evenly distributed allocation of mobile agents, where the PCP has provided equidistant agent spacing for each flow. At this same time (450 time steps), the flow \mathcal{F}_3 activates, initiating a reconfiguration by the ICP to optimize the newly added flow, as in Fig. 3c, noting that initially in Fig. 3b, \mathcal{F}_3 is poorly served by the network configuration. Finally, flow \mathcal{F}_2 is deactivated, forcing another reconfiguration yielding the equilibrium shown in Fig. 3d. The per-flow utility over the simulation, given for a flow $i \in \mathcal{I}_F$ by $\sum_{(j,k) \in \mathcal{E} \mid i \in \mathcal{M}_j \cap \mathcal{M}_k} w_{ij}$ (the sum of the link utilities associated with each flow), is depicted in Fig. 4. To better illustrate the dynamics of our proposed algorithms, we direct the reader to the media attachment for the associated simulation video.

VI. CONCLUSION

In this paper, we illustrated a novel hybrid architecture for command, control, and coordination of networked robots for sensing and information routing applications, called INSPIRE (for INformation and Sensing driven Physically REconfigurable robotic network). INSPIRE provides of two control levels, namely Information Control Plane and Physical Control Plane, so that a feedback between information and sensing needs and robotic configuration is established. An instantiation was provided as a proof of concept where a mobile robotic network is dynamically reconfigured to ensure high quality routes between static wireless nodes, which act as source/destination pairs for information flow. Future work will focus on the validation of the proposed architecture in a real-world scenario having mobile robotic interaction with a sensor network testbed.

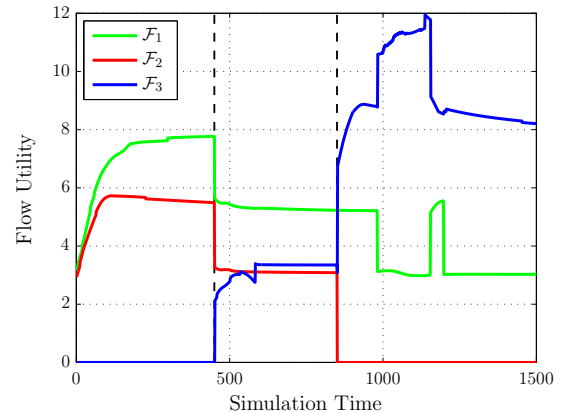


Fig. 4. Flow utilities for the simulated execution described in Section V.

REFERENCES

- [1] G. Wang, G. Cao, P. Berman, and T. La Porta, "Bidding protocols for deploying mobile sensors," *IEEE Transactions on Mobile Computing*, vol. 6, no. 5, pp. 563–576, 2007.
- [2] A. Gasparri, B. Krishnamachari, and G. S. Sukhatme, "A framework for multi-robot node coverage in sensor networks," *Annals of Mathematics and Artificial Intelligence*, vol. 52, no. 2-4, pp. 281–305, 2008.
- [3] M. M. Zavlanos and G. J. Pappas, "Distributed connectivity control of mobile networks," *IEEE Transactions on Robotics*, vol. 24, no. 6, pp. 1416–1428, 2008.
- [4] L. Sabattini, C. Secchi, N. Chopra, and A. Gasparri, "Distributed control of multirobot systems with global connectivity maintenance," *IEEE Transactions on Robotics*, vol. 29, no. 5, pp. 1326–1332, Oct 2013.
- [5] N. Chatzipanagiotis, M. M. Zavlanos, and A. Petropulu, "A distributed algorithm for cooperative relay beamforming," in *ACC*, 2013.
- [6] D. K. Goldenberg, J. Lin, A. S. Morse, B. E. Rosen, and Y. R. Yang, "Towards mobility as a network control primitive," in *MobiHoc '04*. ACM, 2004, pp. 163–174.
- [7] Y. Yan and Y. Mostofi, "Robotic router formation in realistic communication environments," *IEEE Transactions on Robotics*, vol. 28, no. 4, pp. 810–827, 2012.
- [8] M. Ji and M. Egerstedt, "Distributed Coordination Control of Multiagent Systems While Preserving Connectedness," *IEEE Transactions on Robotics*, vol. 23, no. 4, pp. 693–703, 2007.
- [9] M. Z. Zamalloa and B. Krishnamachari, "An analysis of unreliability and asymmetry in low-power wireless links," *ACM Trans. Sen. Netw.*, vol. 3, no. 2, Jun. 2007.
- [10] R. Williams and G. Sukhatme, "Constrained interaction and coordination in proximity-limited multiagent systems," *IEEE Transactions on Robotics*, pp. 1–15, 2013.
- [11] D. Dimarogonas and K. Kyriakopoulos, "Inverse agreement protocols with application to distributed multi-agent dispersion," *IEEE Transactions on Automatic Control*, vol. 54, no. 3, pp. 657–663, 2009.